Stem Cell Reports
Article

ISSCR

OPEN ACCESS

TGF-β Signaling Accelerates Senescence of Human Bone-Derived CD271 and SSEA-4 Double-Positive Mesenchymal Stromal Cells

Hiroshi Kawamura,[1,2] Ryusuke Nakatsuka,[1] Yoshikazu Matsuoka,[1] Keisuke Sumide,[1] Tatsuya Fujioka,[1] Hiroaki Asano,[3] Hirokazu Iida,[2] and Yoshiaki Sonoda[1,*]

[1]Department of Stem Cell Biology and Regenerative Medicine, Graduate School of Medical Science, Kansai Medical University, Hirakata, Osaka 573-1010, Japan
[2]Department of Orthopaedic Surgery, Kansai Medical University, Hirakata, Osaka, Japan
[3]School of Nursing, Kyoto Prefectural University of Medicine, Kyoto, Japan
*Correspondence: sonoda@hirakata.kmu.ac.jp
https://doi.org/10.1016/j.stemcr.2018.01.030

SUMMARY

It is generally thought that the proliferative capacity and differentiation potential of somatic stem cells, including mesenchymal stromal/stem cells (MSCs) and hematopoietic stem cells, decline with age. We investigated the effects of aging on human bone-derived MSCs expressing CD271 and SSEA-4 (double-positive MSCs [DPMSCs]). The percentages of DPMSCs in bone tissue decreased significantly with age. The DPMSCs from elderly patients (old DPMSCs) showed cellular senescence, which was evidenced by low growth potential, high senescence-associated β-galactosidase activity, and elevated p16 and p21 CDK inhibitor levels. Moreover, old DPMSCs showed weak osteogenic differentiation potential and less hematopoiesis-supporting activity in comparison with young DPMSCs. Interestingly, the addition of transforming growth factor β2 (TGF-β2) induced cellular senescence in young DPMSCs. With the exception of the adipogenic differentiation potential, all of the aging phenomena observed in old DPMSCs were reversed by the addition of anti-TGF-β antibodies. These results suggest that, in part, old DPMSCs accelerate cellular senescence through TGF-β signaling.

INTRODUCTION

It is well documented that the proliferative capacity and differentiation potential of somatic stem cells, including mesenchymal stromal/stem cells (MSCs) and hematopoietic stem cells (HSCs), decline with age (Oh et al., 2014; Allsopp et al., 2003; Nakamura-Ishizu and Suda, 2014). This process is included in the concept of senescence. However, the process of stem cell senescence remains elusive. Thus, it is important to elucidate the fundamental molecular mechanisms that regulate the cellular functions of stem cells, such as MSCs and HSCs, in order to understand their aging process.

From another point of view, HSCs are thought to be maintained in the specialized bone marrow (BM) microenvironment, also known as the HSC niche (Morrison and Scadden, 2014; Méndez-Ferrer et al., 2010). Collectively, it is considered that the aging of niche cells may affect the cellular senescence of HSCs in terms of their self-renewal activity, and their proliferation and differentiation abilities (Mendelson and Frenette, 2014). In fact, it was reported that aged MSCs exerted weak osteogenic differentiation potential and enhanced adipogenic differentiation potential, both of which are evidence of cellular senescence (Liu et al., 2015). Moreover, aged MSCs produced various tissue-aging stimulating factors. These bioactive mediators are thought to be a component of the senescence-associated secretory phenotype (SASP) (Acosta et al., 2013). The SASP causes an inflammatory response as well as the cell-cycle arrest of surrounding cells through a paracrine mechanism (Acosta et al., 2013). However, the relationship between individual aging and the cellular senescence of MSCs is still unclear. Furthermore, the mechanism of the cellular senescence of MSCs and the HSC-supporting activity of aged human MSCs have remained elusive until now.

Recently, we succeeded in identifying/establishing human BM-derived MSCs that express CD271 and SSEA-4 (double-positive MSCs [DPMSCs]) (Matsuoka et al., 2015). The DPMSCs had an ability to differentiate into mesenchymal cell lineages and supported the activity of human cord blood (CB)-derived CD34-positive and negative ($CD34^{+/-}$) HSCs *in vitro*. These DPMSCs expressed higher levels of HSC-supportive genes, including *CXCL12* and *FOXC1* (Omatsu et al., 2014) and showed the higher supporting ability of human CB-derived $CD34^{-}$ HSCs (Matsuoka et al., 2015). It is well documented that steady-state hematopoiesis is sustained by HSCs and niche cells, including DPMSCs and various cytokines (Morrison and Scadden, 2014; Méndez-Ferrer et al., 2010; Lapidot et al., 2005; Wilson and Trumpp, 2006; Smith and Calvi, 2013). Thus, it would be interesting to know how aging affects the niche function of DPMSCs.

In this study, we succeeded in establishing human bone-derived DPMSCs from two different donor groups: young and elderly adults. We then investigated the effects of aging on the functions of human bone-derived DPMSCs *in vitro* and *in vivo* to understand the basic mechanisms of cellular senescence. We found that transforming growth factor β2

(TGF-β2) is one of the candidate factors for the aging of DPMSCs. Interestingly, with the exception of the adipogenic differentiation potential, all of the aging phenomena observed in old DPMSCs were reversed by the addition of anti-TGF-β antibodies (1D11). These results suggest that, in part, old DPMSCs accelerate cellular senescence through TGF-β signaling.

RESULTS

Anatomical Distribution and Proportion of Bone-Derived 11Lin$^-$CD45$^-$CD271$^+$SSEA-4$^+$ Cells

First, we analyzed/compared the proportion of 11Lin$^-$CD45$^-$CD271$^+$SSEA-4$^+$ cells in human femoral neck bone tissues and their BM. The BM cells residing in the bone tissues were collected by vigorous washing. Bone-derived cells were collected from the remaining bone tissue after enzymatic treatment with collagenase and dispase (see Supplemental Experimental Procedures). As shown in Figure S1A, the proportion of 11Lin$^-$CD45$^-$CD271$^+$SSEA-4$^+$ cells in bone-derived cells was greater than that of BM cells. Next, we compared the proportions of 11Lin$^-$CD45$^-$CD271$^+$SSEA-4$^+$ cells in the human femoral neck, femoral head, and acetabulum. As clearly shown in Figure S1B, the proportion of 11Lin$^-$CD45$^-$CD271$^+$SSEA-4$^+$ cells in the femoral neck was higher than the proportions in the femoral head and acetabulum. Based on these findings, we used human femoral neck-derived 11Lin$^-$CD45$^-$CD271$^+$SSEA-4$^+$ cells in the following experiments.

Isolation of Bone-Derived 11Lin$^-$CD45$^-$CD271$^{+/-}$SSEA-4$^{+/-}$ Cells from Young and Elderly Patients and Establishment of Bone-Derived Mesenchymal Stromal/Stem Cells

Human femoral neck bone tissue samples are shown in Figure S2A. As the figure clearly shows, the depth of the cortical bone of the elderly patient was thinner than that of the young patient. In addition, the degree of osteoporotic change in the cancellous bone (Cn) was more severe in the elderly patient than in the young patient. As shown in Figure S2B, the young patient's bone-derived 11Lin$^-$CD45$^-$ cells were further subdivided into CD271$^-$SSEA-4$^+$ (SSEA-4 single-positive; SSEA-4 SP, R4), CD271$^+$SSEA-4$^+$ (double-positive; DP, R5), CD271$^-$SSEA-4$^-$ (double-negative; DN, R6) and CD271$^+$SSEA-4$^-$ (CD271 single-positive; CD271 SP, R7) fractions according to their expression levels of CD271 and SSEA-4, as previously reported (Matsuoka et al., 2015). These four cell fractions were cultured in α-minimum essential medium (α-MEM) with 10% fetal bovine serum (FBS) at 37°C with 5% CO_2. We then succeeded in establishing three MSC lines from the R5, R6, and R7 fractions, respectively (Figure S2Cb, c, and d). These three MSC lines showed a similar spindle-shaped morphology. Among them, MSCs from the DN fraction showed poor proliferation. We finally succeeded in establishing DPMSC lines from 3 out of 3 young patients and 3 out of 8 elderly patients (Table S1).

We then analyzed the cell-surface marker expression of young and old DPMSCs. Both of the DPMSCs expressed known MSC markers, including CD29, CD44, CD73, CD90, and CD105 (Figure S3Aa). Both DPMSCs also expressed human leukocyte antigen (HLA)-ABC, but not HLA-DR. In contrast, none of these DPMSCs expressed the endothelial/hematopoietic cell markers, including CD31, CD34, CD41, CD45, and CD56 (Figure S3Aa). Interestingly, both DPMSCs expressed perivascular cell markers, including CD146, neuron-glial 2 (NG2), platelet-derived growth factor receptor α (PDGFRα), and PDGFRβ (Figure S3Ab). qRT-PCR confirmed the expression of perivascular cell marker genes, including *CSPG4*, *MCAM*, *PDGFRA*, *PDGFRB*, *ACTA2*, and *NES* (Figure S4). The expression of CD271 on old DPMSCs was downregulated during *in vitro* passages (Figure S3B). Conversely, the expression of SSEA-4 on both young and old DPMSCs was unchanged until passage 4.

Percentages of Bone-Derived CD271$^{+/-}$SSEA-4$^{+/-}$ Cells in Young and Elderly Patients

Next, we compared the percentages of bone-derived CD271$^{+/-}$SSEA-4$^{+/-}$ cells in young and elderly patients. Representative scattergrams of the expression of CD271 and SSEA-4 on bone-derived 11Lin$^-$CD45$^-$ cells from young and elderly patients are shown in Figure 1A. The percentages of CD271$^-$SSEA-4$^+$ (R4), CD271$^-$SSEA-4$^-$ (R6), and CD271$^+$SSEA-4$^-$ (R7) cells were comparable (Figure 1B and Table S1). Interestingly, the percentage of elderly patient-derived CD271$^+$SSEA-4$^+$ (R5) cells was significantly decreased in comparison with that in young patient-derived cells (Figure 1Bb). However, we succeeded in establishing bone-derived DPMSCs from both young and elderly patients. As we recently reported (Matsuoka et al., 2015), human BM-derived DPMSCs exerted potent HSC-supportive activity. We therefore focused on the bone-derived DPMSCs from young and elderly patients and analyzed their stem cell characteristics from the viewpoint of cellular senescence.

Stem Cell Characteristics of CD271$^+$SSEA-4$^+$ MSCs Established from the Bone Tissue of Young and Elderly Patients

As shown in Figure 2Aa, all three DPMSCs established from young patients (young DPMSCs) showed continuous growth curves until passage 16, at which point they plateaued. In contrast, two of the three DPMSC lines established from elderly patients (old DPMSCs) showed

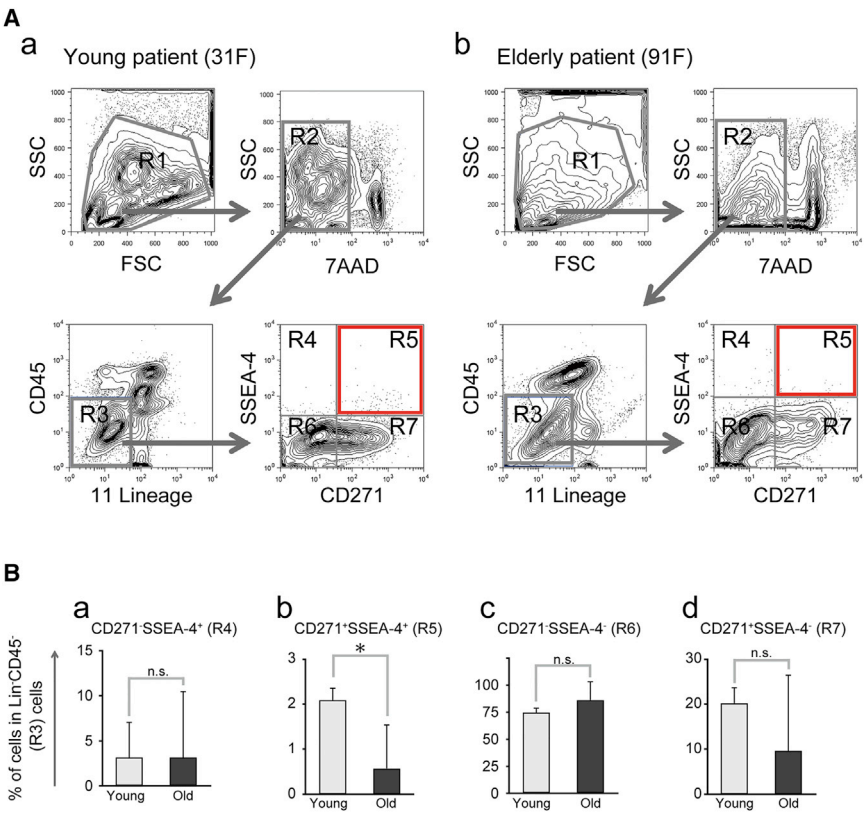

Figure 1. Qualitative Assessment of $CD271^{+/-}SSEA\text{-}4^{+/-}$ Cells Residing in the Bone Tissue of Young and Elderly Patients

(A) Representative flow cytometry (FCM) profiles of the distribution of $CD271^{+/-}$ $SSEA\text{-}4^{+/-}$ cells residing in bone tissue derived from (a) a young female patient (31 years old, indicated as "31F") and (b) an elderly female patient (91 years old, indicated as "91F"). The gates (R1 to R7) were set on each scattergram (see also Figures S1 and S2B). Cells in R5 fraction are indicated by the red square.

(B) The percentages of (a) $CD271^{-}SSEA4^{+}$ (R4), (b) $CD271^{+}SSEA4^{+}$ (R5), (c) $CD271^{-}$ $SSEA4^{-}$ (R6), and (d) $CD271^{+}SSEA4^{-}$ (R7) fraction in cells derived from the bone tissue of three young (Young) and eight elderly (Old) patients are shown. Each bar represents the mean ± SD of FCM data obtained from three young and eight elderly patients. These data were evaluated by Welch's t test. *$p < 0.05$; n.s., not significant.

See also Table S1.

continuous growth curves until only passage 11; they then plateaued and stopped proliferating at passage 12. One DPMSC line established from an elderly patient (91 years old) showed poor proliferation ability and stopped proliferating at passage 4. These results clearly demonstrated that the young DPMSCs had a growth advantage in comparison with the old DPMSCs.

Next, we compared the growth curves of three types of MSCs (DPMSCs, CD271SP MSCs, and DN MSCs) established from one young (28F) patient and one old (80F) patient. As shown in Figure 2Ab, the three types of young MSC lines showed continuous growth curves until passage 12. However, the young DPMSCs showed a growth advantage in comparison with the two other types of MSC lines. Two old MSC lines (DPMSCs and CD271SP MSCs) both showed continuous growth curves until passage 11 (Figure 2Ac). Again, old DPMSCs showed a growth advantage in comparison with CD271SP MSCs. In contrast, the old DN MSCs showed poor proliferation ability and their proliferation stopped at passage 9.

From another point of view, the aforementioned growth curve of old DPMSCs suggests their early cellular senescence. Thus, we analyzed the expression of the senescence-associated β-galactosidase (β-gal) activity in young and old DPMSCs (Figure 2B). At passage 4, the mean percentages of β-gal-positive cells in young and old DPMSCs were 1.3% and 20.6%, respectively. At passage 9, the mean percentage of β-gal-positive cells was still 3.1% in young DPMSCs; however, it dramatically increased to 83.2% in old DPMSCs. We then analyzed the expression of cyclin-dependent kinase (CDK) inhibitors, including p16 and p21, which are known to play an important role in arresting the cell cycle in the G_1 phase of stem cells upon a variety of stimuli (Collado et al., 2007; van Deursen, 2014; Gil and Peters, 2006). As expected, old DPMSCs expressed significantly higher levels of *P16* and *P21* in comparison with young DPMSCs (Figure 2C).

Osteogenic, Adipogenic, and Chondrogenic Differentiation Potential of Established Young and Old DPMSCs

We assessed the differentiation potential of established young and old DPMSCs. The DPMSCs (passage 4) were induced to differentiate into osteogenic, adipogenic, and chondrogenic lineages (Figure 3A). We found that the young and old DPMSCs could differentiate into all three lineages. However, the young DPMSCs showed a significantly higher osteogenic differentiation capacity in comparison with old DPMSCs (Figure 3Ba and b). In contrast, old DPMSCs showed significantly higher adipogenic differentiation

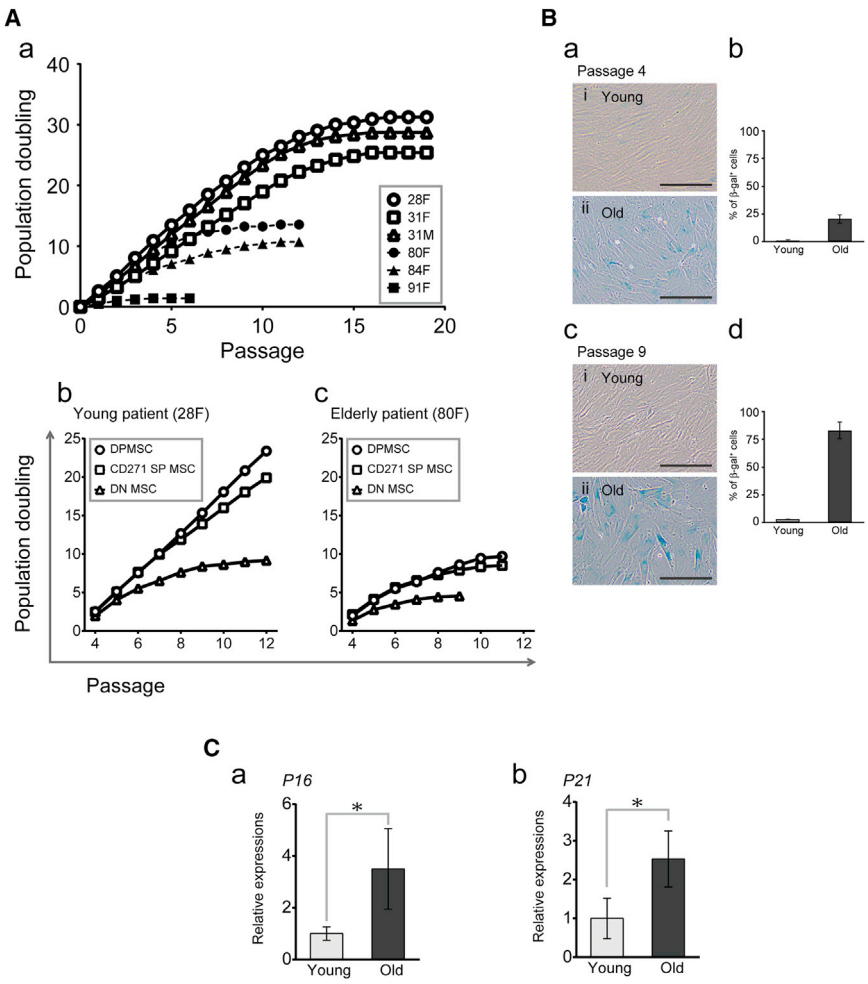

Figure 2. Cellular Senescence in Bone Tissue-Derived CD271 and SSEA-4 Double-Positive Mesenchymal Stromal Cells from Young and Elderly Patients

(A) Cell growth potential of bone-derived DPMSCs from young and elderly patients. The population doubling levels of each cell were calculated with cell counts at every passage. (a) Open symbols indicate DPMSCs from three young patients (28F, circles; 31F, squares; 31M, triangles) and closed symbols indicate those from three elderly patients (80F, circles; 84F, triangles; 91F, squares). The cell growth potential of three types of bone-derived (b) young and (c) old MSCs, including DPMSCs, CD271SP MSCs, and DN MSCs, was established from one young patient (28F) or one elderly patient (80F), respectively.

(B) We used two young and two old DPMSC lines. Representative phase-contrast images of young DPMSCs (a-i and c-i) and old DPMSCs (a-ii and c-ii). Old DPMSCs showed an enlarged and flattened morphology, which are characteristics of senescent cells. These cells were stained with SA-β-gal and photomicrographs were taken. Scale bar, 200 μm. (b and d) The percentages of β-gal$^+$ DPMSCs in relation to the total number of cells in the five pictured microscopy fields at P4 and P9 were analyzed. Error bars represent the mean ± SD of 10 measurements (5 per one young or old DPMSC line) in two independent experiments. Data were evaluated by Welch's t test.

(C) We used three young and three old DPMSC lines. qRT-PCR of the expression of (a) *P16* mRNA and (b) *P21* mRNA between young and old DPMSCs was performed. The signal intensities of old DPMSCs (Old) were compared with those of young DPMSCs (Young). Error bars represent the mean ± SD of six (*P16*) and three (*P21*) independent measurements. Data were evaluated by Welch's t test. *p < 0.05.
See also Figures S3 and S6B.

capacity in comparison with young DPMSCs (Figure 3Bc and d). Interestingly, the young DPMSCs expressed significantly higher levels of *RUNX2* (an osteogenic gene) in comparison with old DPMSCs (Figure 3Ca). On the other hand, the expression levels of *PPARG2* (an adipogenic gene) (Figure 3Cb) and *SOX9* (an osteo-chondrogenic gene) (Figure 3Cc) were comparable between young and old DPMSCs.

Hematopoiesis-Supporting Abilities of Young and Old DPMSCs: Effects of the Direct Adhesion of DPMSCs to Hematopoietic Cells

The hematopoiesis-supportive abilities of young and old DPMSCs were first assessed using a co-culture system. In these experiments, we used sorted human CB-derived 18Lin$^-$CD34$^+$CD38$^-$CD133$^+$ (abbreviated as 34$^+$38$^-$133$^+$) cells (Figure 4Aa, R5) as a target cell population, which contained primitive long-term repopulating HSCs, as previously reported (Takahashi et al., 2014). The young and old DPMSCs (passage 4) were seeded and cultured for 7 days before the start of co-culturing. The 34$^+$38$^-$133$^+$ cells were cultured with or without feeder DPMSCs for 7 days in serum-free medium with a cocktail of cytokines (Figure 4Ab–e). After co-culturing, the cells were collected, and the hematopoiesis-supportive abilities of the DPMSCs *in vitro* were assessed by cell proliferation/differentiation assays.

In the co-cultures of 34$^+$38$^-$133$^+$ cells, the numbers of cells were increased with young DPMSCs (130- to 200-fold) and old DPMSCs (80- to 130-fold) (Figure 4Ba). Both young and old DPMSCs supported significantly higher numbers of cells in comparison with the stroma-free

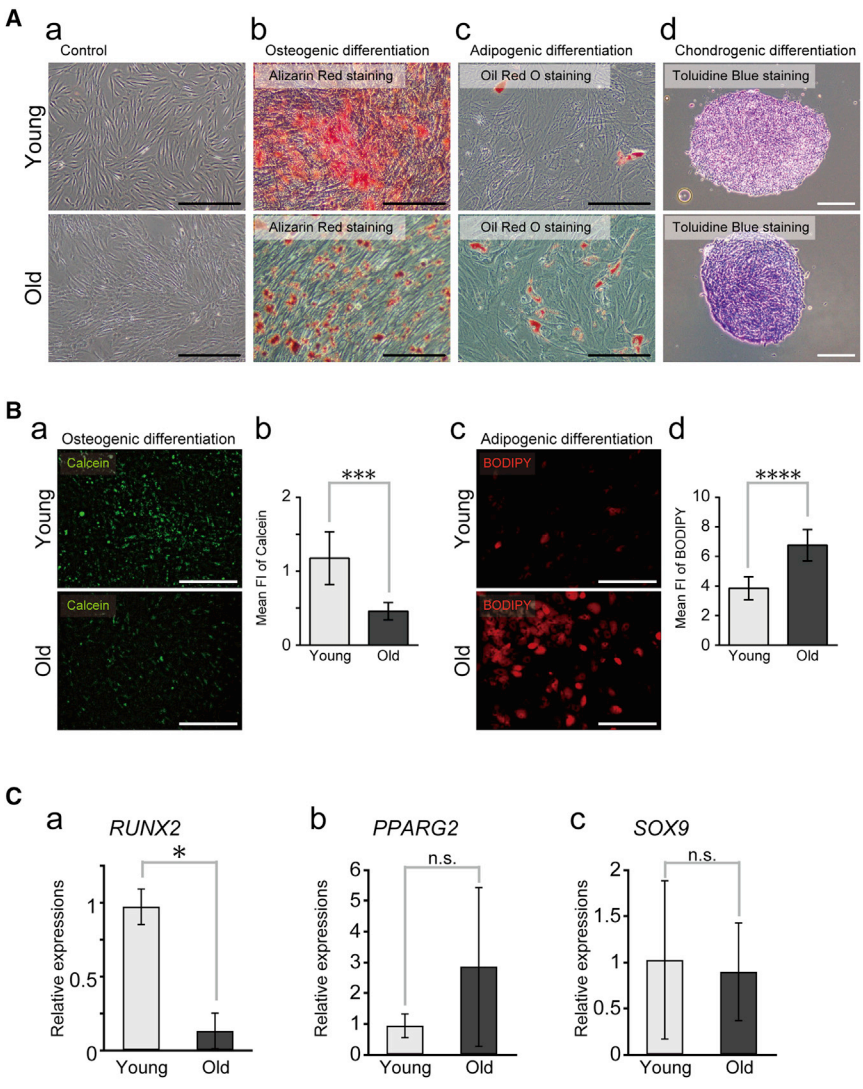

Figure 3. Differentiation Potential of Bone Tissue-Derived DPMSCs from Young and Elderly Patients

(A) Representative photomicrographs of the induction of the (a) control cultures at passage 4, (b) osteogenic (Alizarin red S), (c) adipogenic (oil red O), and (d) chondrogenic (toluidine blue) differentiation of young (upper panel) and old (lower panel) DPMSCs. Scale bars, 500 μm (a–c) and 200 μm (d).

(B) We used three young and three old DPMSC lines for quantitative evaluation of the osteogenic and adipogenic differentiation potentials of young and old DPMSCs. Representative fluorescence images of cellular calcium deposition staining using calcein (a) and lipid droplets staining using BODIPY (c) in young (upper panel) and old (lower panel) DPMSCs are shown. Scale bars, 500 μm. The mean intensity of (b) calcein and (d) BODIPY fluorescence of the differentiated DPMSCs in the three pictured fields of each DPMSC line were analyzed by fluorescence microscopy. Data show the mean fluorescence intensity (MFI) of three young or old DPMSC lines. Error bars represent the mean ± SD of nine measurements (3 per one young or old DPMSC line) in three independent experiments. Data were evaluated by Welch's t test. ***$p < 0.001$, ****$p < 0.0001$.

(C) We used three young and three old DPMSC lines. The expression of osteogenic, adipogenic, and chondrogenic differentiation-related genes in steady-state young and old DPMSCs are shown. These signal intensities of old DPMSCs (Old) were compared with those of young DPMSCs (Young). Error bars represent the mean ± SD of three independent measurements. Data were evaluated by Welch's t test. *$p < 0.05$; n.s., not significant.

See also Figure S3.

control (mean, 53-fold). Interestingly, young DPMSCs supported significantly higher numbers of cells in comparison with old DPMSCs. The mean percentages of $CD34^+$ cells after 7 days of co-culturing $34^+38^-133^+$ cells with young or old DPMSCs (33.9% or 30.9%, respectively) were significantly higher than that of the stroma-free control (17.9%) (Figure 4Bb). As a result, the mean absolute numbers of $CD34^+$ cells after 7 days of co-culturing $34^+38^-133^+$ cells with young or old DPMSCs (160×10^3 or 89×10^3, respectively) were significantly higher than that of the stroma-free controls (28×10^3) (Figure 4Bc). Moreover, there was a significant difference between the co-cultures with young and old DPMSCs.

Next, we analyzed the contact-independent hematopoiesis-supportive abilities of young and old DPMSCs using a transwell system. The $34^+38^-133^+$ cells were seeded directly or indirectly onto young and old DPMSCs feeders using transwell culture insert. The $34^+38^-133^+$ cells that were cultured without feeders were used as a stroma-free control. In the presence of a transwell, the magnitude of cellular proliferation was reduced in both of the co-cultures. Namely, the numbers of cells increased with young DPMSCs (70- to 100-fold) and old DPMSCs (50- to 70-fold). However, both young and old DPMSCs supported higher numbers of cells in comparison with the stroma-free control (mean, 40-fold) (Figure 4Ca). Notably, there

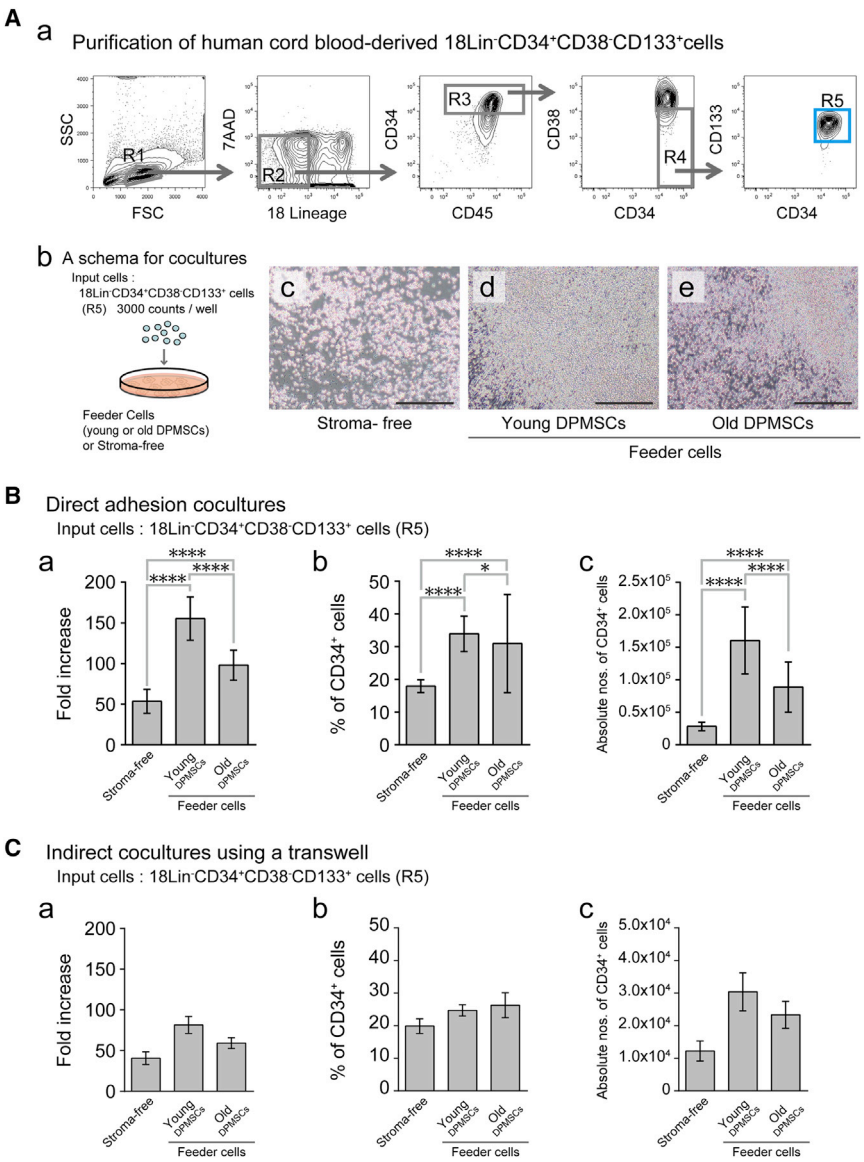

Figure 4. Human Hematopoietic Stem/Progenitor Cell-Supporting Abilities of Bone Tissue-Derived DPMSCs from Young and Elderly Patients

(A) (a) Representative FCM profile of CB-derived 18Lin$^-$CD34$^+$CD38$^-$CD133$^+$ cells (R5) is shown. (b) Three thousand CB-derived R5 cells were co-cultured with or without young DPMSCs (Young) and old DPMSCs (Old), and representative photomicrographs taken on day 7 are shown (c–e). Scale bar, 500 μm.

(B) We used three young and three old DPMSC lines. Hematopoietic cells recovered from co-cultures were further analyzed to determine (a) the fold increase in the total numbers of cells, (b) the percentages of CD34$^+$ cells, and (c) the absolute number of CD34$^+$ cells. We used three culture dishes per one young or old DPMSC line. Error bars represent the mean ± SD of nine culture dishes in three independent experiments. Data were evaluated by two-way ANOVA test with Tukey's multiple comparison procedure. *$p < 0.05$, ****$p < 0.0001$.

(C) We used two young and two old DPMSC lines. Three thousand CB-derived R5 cells were co-cultured with or without young and old DPMSCs in the presence of a transwell. The hematopoietic cells recovered from co-cultures were further analyzed to determine (a) the fold increase in the total numbers of cells, (b) the percentages of CD34$^+$ cells, and (c) the absolute number of CD34$^+$ cells. We used three culture dishes per one young or old DPMSC line. Error bars represent the mean ± SD of six culture dishes in two independent experiments. Data were evaluated by two-way ANOVA test with Tukey's multiple comparison procedure.

See also Figures S4, S5, and S7.

seemed to be a difference between the co-cultures with young and old DPMSCs even in the presence of a transwell. Interestingly, the mean absolute numbers of CD34$^+$ cells after 7 days of co-culturing 34$^+$38$^-$133$^+$ cells with young and old DPMSCs (30×10^3 and 23×10^3) seemed to be higher than the mean absolute numbers of CD34$^+$ cells in stroma-free controls (12×10^3) (Figure 4Cc). The mean absolute numbers of CD34$^+$ cells after 7 days of co-culturing 34$^+$38$^-$133$^+$ cells with young DPMSCs tended to be higher than that of old DPMSCs, albeit not to a significant degree (Figure 4Cc). These results demonstrated that the contact of the target cells with young and old DPMSCs exerted significant hematopoiesis-supporting abilities. However, this contact was not essential for the hematopoiesis-supporting abilities of either young or old DPMSCs. In addition, it was suggested that some soluble factors secreted/produced by young and old DPMSCs may play an important role in the hematopoiesis-supporting abilities.

Next, we performed co-culturing experiments in which 34$^+$38$^-$133$^+$ cells were co-cultured with three types of bone-derived MSCs (DPMSCs, CD271SP MSCs, and DN MSCs) for 2 weeks. As shown in Figure S5A, all three types of young and old MSCs supported significantly higher absolute numbers of CD45$^+$ cells (a to c) and CD34$^+$ cells (d to f) in comparison with the stroma-free cultures. After 2 weeks of co-culture, the absolute numbers of CD45$^+$ and CD34$^+$ cells were greater in comparison with the

numbers after 1 week of co-culturing. Very interestingly, all three types of young MSCs supported significantly higher numbers of $CD34^+$ cells in comparison with the three types of old MSCs. Next, we analyzed the effects of all three types of MSCs on the *ex vivo* expansion of colony-forming cells (CFCs). Consistent with the effects on the absolute numbers of $CD34^+$ cells, the same trends were observed in the co-cultures with all three types of MSCs (Figure S5B). We then analyzed the proportions of colony types, including CFU-GM, BFU-E, and CFU-Mix, in the co-cultures with the three types of MSCs. After 1 week of co-cultures, the proportions of BFU-E in the co-cultures with all three types of young MSCs were significantly higher than those with the three types of old MSCs. After 2 weeks of co-culturing, however, the proportions of CFU-GM were increased in the co-cultures with all three types of young and old MSCs (Figure S5C). Collectively, these results suggest that the young DPMSCs exerted more potent hematopoietic progenitor cell (HPC)-supporting abilities in comparison with old DPMSCs through direct and/or indirect mechanisms.

Expression Profiles of Hematopoiesis-Supportive Genes and Perivascular Cell Marker Genes in Young and Old DPMSCs

We then analyzed the differences in the hematopoiesis-supportive gene expression profiles between young and old DPMSCs. These genes have already been reported to be expressed in mouse and human HSC niche cells (Ren et al., 2011). As shown in Figure S4, the expression of *IGF2*, *TGFB3*, *CXCL12*, and *FOXC1* in young DPMSCs tended to be higher than in old DPMSCs, albeit not to a significant degree. The expression of other hematopoiesis-supportive genes, including *WNT3A*, *JAG1*, *ANGPT1*, *TGFB1*, and *FGF2*, was comparable in young and old DPMSCs. Among the perivascular cell marker genes, including *CSPG4*, *MCAM*, *PDGFRA*, *PDGFRB*, *ACTA2*, and *NES*, the expression of *PDGFRB* in young DPMSCs was significantly higher than that in old DPMSCs.

Hematopoiesis-Supporting Abilities of Young and Old DPMSCs as Evaluated by SCID-Repopulating Cell Activity

The SCID-repopulating cell (SRC) activities of cultured $34^+38^-133^+$ cells were assessed at 20 weeks after transplantation (Table S2). Specified numbers of cells recovered from the co-cultures with or without DPMSCs were transplanted into NOG mice using the intra-bone marrow injection (IBMI) method (Table S2). As shown in Figure 5Aa, all of the five mice that received stroma-free cultured cells showed human $CD45^+$ cell engraftment in the left tibia (median, 3.7%). All of the five mice that received co-cultured cells with young and old DPMSCs showed human $CD45^+$ cell engraftment in the left tibia (median, 43.1% and 10.5%, respectively). Interestingly, the median repopulation level of $CD45^+$ cells in the five mice that received cells co-cultured with young DPMSCs was significantly higher than that of the mice that received cells from stroma-free cultures. In the peripheral blood (PB), the repopulation levels of $CD45^+$ cells in the mice that received cells co-cultured with young and old DPMSCs (median, 4.2% and 11.7%, respectively) were also significantly higher in comparison with that of the mice that received cells from stroma-free cultures (median, 0.0%). We then analyzed the multilineage differentiation capacities of SRCs supported by three culture conditions. As shown in Figure 5Ab–g, most of the engrafted mice showed lympho-myeloid repopulation, including $CD34^+$, $CD19^+$, $CD33^+$, $CD11b^+$, and $CD14^+$ cells. We also detected $CD3^+$ T-lymphoid cells in the thymi of some of the mice.

We then we performed secondary transplantation. As shown in Figure 5B, all three types of BM cells recovered from all mice that received stroma-free cultured cells and cells co-cultured with young and old DPMSCs contained significant numbers of $18Lin^-CD34^+CD38^-$ cells. As shown in Figure 5C and Table S2, 5 of 10 mice that received BM cells obtained from primary recipient mice that received cells recovered from the cells co-cultured with young and old DPMSCs were respectively repopulated with human $CD45^+$ cells with multilineage differentiation. In contrast, none of the 10 mice that received BM cells obtained from the primary recipient mice that received cells recovered from the stroma-free cultures were repopulated with human $CD45^+$ cells. These findings of the SRC assays suggest that both young and old DPMSCs efficiently support the primary and secondary repopulating abilities of CB-derived multipotential $CD34^+$ SRCs (HSCs) in co-cultures.

Global Gene Expression Analyses of Young and Old DPMSCs

As mentioned above, the difference in the HPC/HSC-supportive ability of young and old DPMSCs may be explained by some soluble factors. To investigate the soluble factors secreted/produced from young and old DPMSCs, we performed a global gene expression analysis using a microarray. First, we compared the gene expression profiles of young and old DPMSCs by a gene set enrichment analysis (GSEA) (Figure S6A). The gene sets enriched in young DPMSCs were those related to cell cycle/mitosis, DNA replication, young cell signature, energy metabolism, and osteogenic differentiation, and so on. The gene sets enriched in old DPMSCs included those related to TGF-β signaling, cell adhesion/migration, adipocyte differentiation, vascular signature, and cell-cycle arrest.

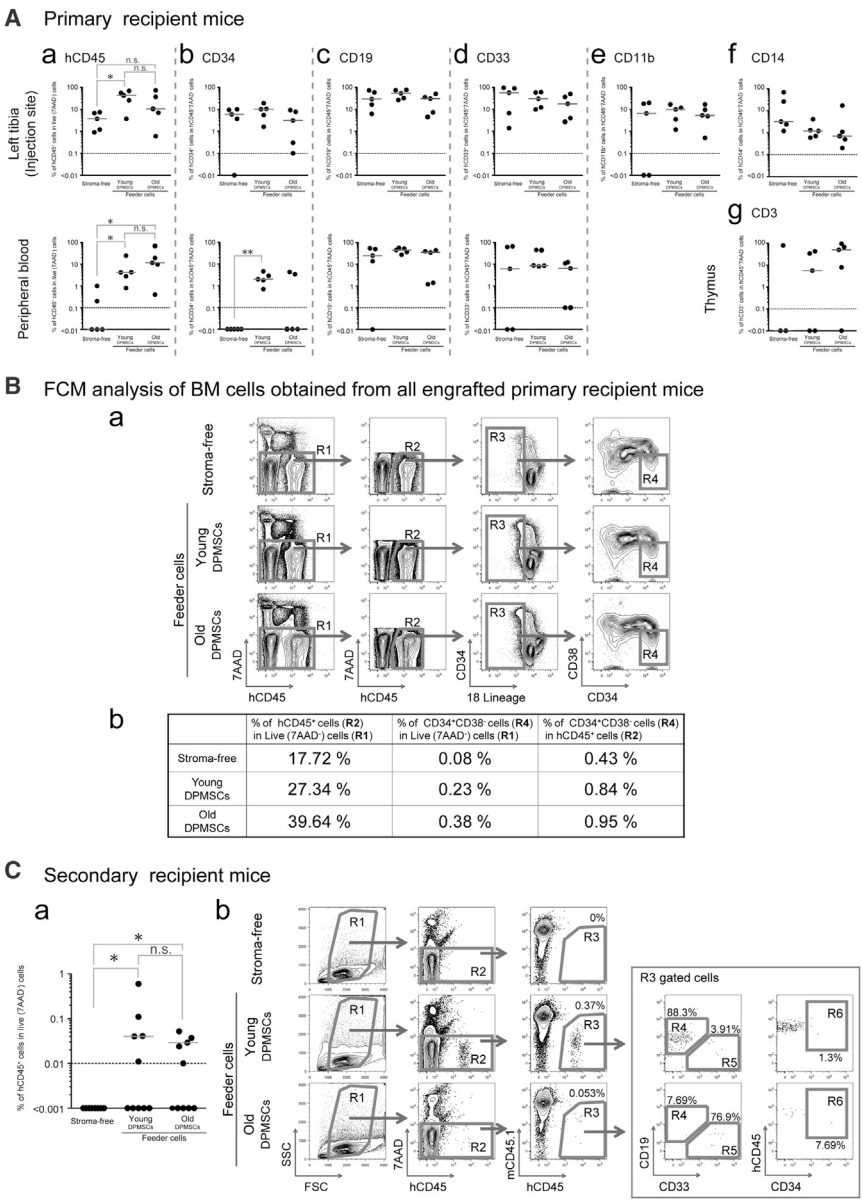

	% of hCD45+ cells (R2) in Live (7AAD-) cells (R1)	% of CD34+CD38- cells (R4) in Live (7AAD-) cells (R1)	% of CD34+CD38- cells (R4) in hCD45+ cells (R2)
Stroma-free	17.72 %	0.08 %	0.43 %
Young DPMSCs	27.34 %	0.23 %	0.84 %
Old DPMSCs	39.64 %	0.38 %	0.95 %

Figure 5. Hematopoiesis-Supportive Effects of Young and Old DPMSCs *In Vivo*

(A) We used one young DPMSC line and one old DPMSC line. The SCID-repopulating cell (SRC)-supportive abilities of young and old DPMSCs were analyzed using *in vitro* co-cultures. The repopulation rates of $CD45^+$ (a), $CD34^+$ (b), $CD19^+$ (c), $CD33^+$ (d), $CD11b^+$ (e), and $CD14^+$ (f) cells in the BM, $CD45^+$ (a), $CD34^+$ (b), $CD19^+$ (c), and $CD33^+$ (d) cells in the PB, and $CD3^+$ cells (g) in the thymus are shown. The horizontal bars indicate the median levels of cells positive for each human hematopoietic marker. Each dot represents the human cell engraftment of an individual mouse. Statistical significance of differences was calculated using Mann-Whitney U tests. *p < 0.05; n.s., not significant.

(B) (a) Representative scattergrams showing the proportions of $18Lin^-CD34^+CD38^-$ cells in the pooled BM cells obtained from all engrafted primary recipient mice shown in (A-a). (b) The percentages of $18Lin^-CD34^+CD38^-$ cells (R4) in R1 and R2 gates are shown.

(C) (a) Secondary repopulating capacities of BM cells obtained from primary recipient mice in three experimental groups, including stroma-free, and co-cultures with young and old DPMSCs. Each dot represents the human cell engraftment of an individual mouse. The horizontal bars indicate the median levels of human $CD45^+$ cells in the engrafted mice. Statistical significance of differences was calculated using Mann-Whitney U tests. *p < 0.05; n.s., not significant. (b) Multilineage repopulation analyses of a representative mouse in each of the three groups are shown.

See also Figure S4 and Table S2.

We then focused on the gene set of genes associated with cell-cycle arrest. As shown in Figure S6Bb, the gene expression levels of CDK inhibitors (including p21, p16, and p15) in the old DPMSCs tended to be high in comparison with those in young DPMSCs. In concert with this tendency, the expression levels of *CDK1* and *CDK2*, which are regulated by p21, and the target genes of the lower pathway, such as *RB1* and *E2F1*, tended to decrease in the old DPMSCs (Figure S6Bc and d). On the other hand, the expression levels of *CDK4* and *CDK6*, which are regulated by p16, were comparable (Figure S6Bc). Next, we selected 138 differentially expressed genes (Table S3) for which the expression levels (signal value) were significantly different (>2-fold difference) from 60,901 probes (Figure 6). Very interestingly, we identified *TGFB2* as a gene that was highly expressed in old DPMSCs in comparison with young DPMSCs (Figures 6 and S6Ba). In contrast, the expression level of *SMAD6*, which suppresses TGF-β signaling, was significantly low, resulting in the enhancement of TGF-β signaling in the old DPMSCs. Moreover, the expression level of the *ID2* gene, which conveys the downstream signal of bone morphogenetic protein, was also significantly low in the old DPMSCs. These results may provide an important clue for elucidating the molecular background that sustains the differential cellular function of young and old DPMSCs.

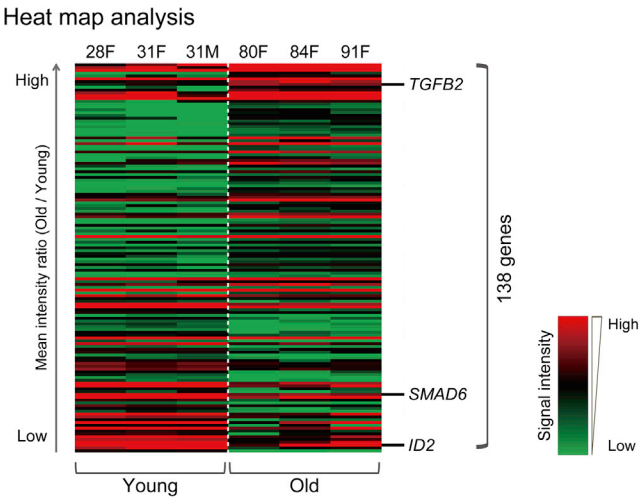

Figure 6. Comparison of the Gene Expression Profiles of Young and Old DPMSCs, as Determined by a Microarray

We used three young and three old DPMSC lines. We performed a microarray analysis once for each young or old DPMSC line (a total of three times). A heatmap created for 138 genes (see also Table S3) for which the signal value extracted from 60,901 probes was found to be significantly different more than two times. The *TGFB2*, *SMAD6*, and *ID2* genes were extracted and are depicted on the right. See also Figure S6.

Effects of TGF-β2 on the Proliferation, Differentiation, and Hematopoiesis-Supporting Abilities of Young and Old DPMSCs *In Vitro*

We analyzed the production of TGF-β2 of young and old DPMSCs. As shown in Figure 7A, old DPMSCs produced a significantly higher level (266 pg/mL) of TGF-β2 in comparison with young DPMSCs (118 pg/mL). Next, we analyzed the effects of TGF-β2 on the proliferation of young DPMSCs in cultures. TGF-β2 suppressed the proliferation of young DPMSCs in a dose-dependent fashion (Figure 7B).

We then analyzed the effects of TGF-β2 or anti-TGF-β monoclonal antibody (mAb) (1D11) on the differentiation capacity of young and old DPMSCs. As shown in Figure 7Ca and b, TGF-β2 strongly suppressed the osteogenic differentiation capacity of both young and old DPMSCs. Interestingly, the addition of 1D11 tended to enhance the osteogenic differentiation capacity of both young and old DPMSCs, albeit not to a significant degree (Figure 7Cc and d). In contrast, the addition of TGF-β2 or 1D11 did not affect the adipogenic differentiation capacity of either young or old DPMSCs (Figure 7D).

Finally, we analyzed the effects of TGF-β2 or 1D11 on the hematopoiesis-supporting capacity of both young and old DPMSCs. In co-cultures of $34^+38^-133^+$ cells with young and old DPMSCs, the numbers of cells increased with both young DPMSCs (100- to 150-fold) and old DPMSCs (80- to 120-fold) (Figure S7A). Both young and old DPMSCs supported higher numbers of cells in comparison with the stroma-free controls (mean, 53-fold). Interestingly, TGF-β2 seemed to inhibit the proliferation of target cells in all three culture conditions (Figure S7A). In contrast, the addition of 1D11 did not show any significant effects on the fold increase of the target cells in any of the three culture conditions.

Consistent with the data shown in Figure 4Cc, after 7 days of co-culturing $34^+38^-133^+$ cells with young and old DPMSCs (80×10^3 and 62×10^3), the mean absolute numbers of $CD34^+$ cells seemed to be higher in comparison with the stroma-free controls (21×10^3) (Figure S7B). The addition of TGF-β2 showed a tendency to reduce the absolute numbers of $CD34^+$ cells in the co-cultures with young and old DPMSCs. Conversely, the addition of 1D11 showed a tendency to enhance the absolute number of $CD34^+$ cells in the co-cultures with young and old DPMSCs, albeit not to a significant degree. Collectively, these results suggest that the hematopoiesis-supporting abilities of young as well as old DPMSCs could be inhibited via TGF-β2 in the BM niche. As shown in Figure 7A, old DPMSCs produced a large amount of TGF-β2 in comparison with young DPMSCs. Thus, it is possible that TGF-β2 may play an important/significant role in hematopoiesis, especially in aged patients.

DISCUSSION

The maintenance of bone homeostasis throughout life depends on the bone remodeling processes, such as bone formation and bone resorption (Seeman and Delmas, 2006). Two types of cells, osteoblasts and osteoclasts, are involved in this process (Seeman and Delmas, 2006). The osteoblasts responsible for bone formation are inducible from MSCs at least *in vitro* (Matsuoka et al., 2015; Tormin et al., 2011). On the other hand, the osteoclasts responsible for bone resorption originate from hematopoietic cells (Xiao et al., 2015). It is well documented that aging has a negative effect on osteogenesis but a positive effect on adipogenesis. Both osteoblasts and adipocytes are derived from bone/BM MSCs at least *in vitro* (Matsuoka et al., 2015; Tormin et al., 2011). Thus, it is conceivable that aging affects the balance of adipogenesis and osteogenesis, as previously reviewed (Bethel et al., 2013). This balance plays an important role in maintaining bone homeostasis as well as steady-state hematopoiesis. It is therefore imperative to clarify the fundamental molecular mechanisms that control this balance in order to understand the cellular senescence of MSCs. However, as it is well known that the population of MSCs is very heterogeneous (Pittenger et al., 1999), it is important to isolate immunophenotypically homogeneous MSC populations

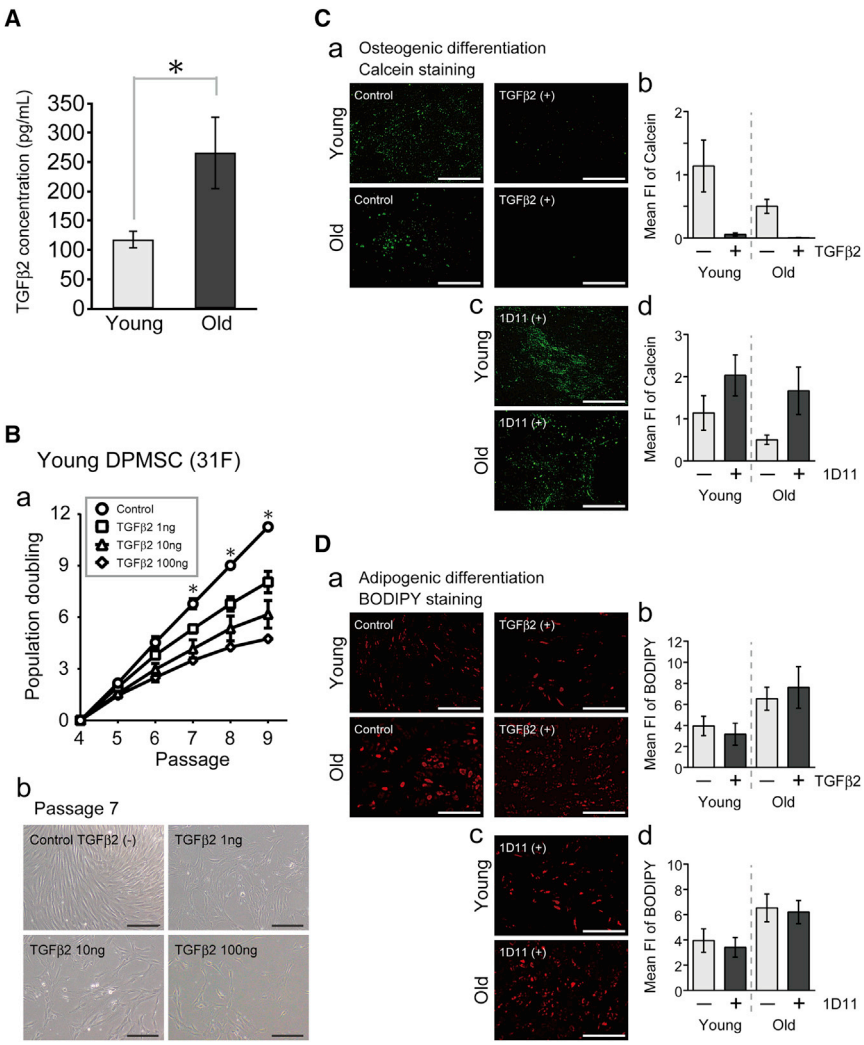

Figure 7. Production of TGF-β2 by Young and Old DPMSCs and the Effects of TGF-β2 on the Proliferation and Differentiation of Young and/or Old DPMSCs in Cultures

(A) We used three young and three old DPMSC lines. The concentration of TGF-β2 protein in the cultures of young and old DPMSCs at passage-4 supernatants was measured by ELISA. Error bars represent the mean ± SD of three independent experiments. Data were evaluated by Welch's t test. *$p < 0.05$.

(B) (a) We performed the same experiments three times using three young DPMSC lines. The growth curve of one representative young DPMSC line (31F) in the presence of various concentrations (1, 10, and 100 ng/mL) of recombinant human TGF-β2 is shown. Each dot represents the mean ± SD of three culture dishes. Data were evaluated by one-way ANOVA with Tukey's multiple comparison procedure. *$p < 0.05$. (b) Representative phase-contrast images of young DPMSCs in the presence or absence of TGF-β2 (1, 10, and 100 ng/mL) at passage 7. Scale bars, 200 μm.

(C and D) We used two young and two old DPMSC lines. The effects of TGF-β2 and anti-TGF-β mAb (1D11) on the osteogenic (C) and adipogenic (D) differentiation potentials of young and old DPMSCs are shown. Representative fluorescence images of cellular calcium deposition staining by calcein (C, a and c) and cellular lipid droplet staining (BODIPY) (D, a and c) in the presence or absence of TGF-β2 (100 ng/mL) or 1D11 (10 μM/mL) are shown. Scale bars, 500 μm. The mean intensity of calcein (C, b and d) and BODIPY (D, b and d) fluorescence of the differentiated DPMSCs of the three pictured fields of each DPMSC line were analyzed by fluorescence microscopy. The data show the MFI of two young or old DPMSC lines. Error bars represent the mean ± SD of six measurements (3 per one young or old DPMSC line) in two independent experiments. Data were evaluated by two-way ANOVA with Tukey's multiple comparison procedure.

See also Figure S7.

to elucidate the aforementioned fundamental molecular mechanism (Matsuoka et al., 2015; Tormin et al., 2011).

Peault and colleagues previously reported a prospective method for isolating $CD146^+$ perivascular cells that were able to support the long-term persistence of human myelo-lymphoid HSCs in co-cultures (Corselli et al., 2013). We recently developed a prospective method for isolating BM-derived MSC populations based on the expression of CD271 and SSEA-4 (Matsuoka et al., 2015). Our established DPMSCs expressed perivascular cell markers, including CD146, α-smooth muscle actin, NG2, PDGFRα and PDGFRβ, and NESTIN (Figures S3 and S4). Thus, the DPMSCs may have some relationship with perivascular cells/pericytes. Indeed, we demonstrated that human BM-derived DPMSCs exerted potent HSC-supporting ability (Matsuoka et al., 2015), as did $CD146^+$ perivascular cells. In this mouse study, nestin-positive MSCs expressing a high level of CXCL12 were found in regions adjacent to the bone or within the BM parenchyma (Méndez-Ferrer et al., 2010). These nestin-positive MSCs significantly co-localized with $Lin^-CD150^+CD48^-$ HSCs, suggesting their function as niche cells. Thus, the DPMSCs have some relevance with mouse nestin-positive MSCs.

In this study, we succeeded in establishing bone-derived young DPMSCs from female/male patients with osteonecrosis. In contrast, we only established bone-derived old

DPMSCs from female patients with osteoarthritis. Interestingly, young DPMSCs exerted more potent effects on the expansion of $CD34^+$ cells and CFCs in comparison with old DPMSCs (Figures S5A and S5B). However, both young and old DPMSCs showed significant HSC-supporting abilities upon primary and secondary transplantation for the SRC assay (Figure 5). These results suggest that hematopoiesis-supporting abilities of young and old DPMSCs may differ between HPCs and HSCs. It was suggested that bone-derived DPMSCs play an important role in bone tissue maintenance, regeneration, and steady-state hematopoiesis. Unexpectedly, the percentages of bone-derived DPMSCs significantly decreased with age (Figure 1 and Table S1), suggesting that this reduction of DPMSCs may cause or be related to the abnormal hematopoiesis observed in elderly patients (Guralnik et al., 2004).

Moreover, old DPMSCs exerted higher adipogenic potential and lower osteogenic potential in comparison with young DPMSCs (Figure 3). In young adults, MSC differentiation favors osteoblastogenesis; however, in elderly adults the differentiation is balanced toward adipogenesis (Bethel et al., 2013). As previously reported, osteoblasts play an important role as a BM niche to support primitive HSCs (Morrison and Scadden, 2014; Méndez-Ferrer et al., 2010). In contrast, adipocytes negatively regulate hematopoiesis (Naveiras et al., 2009). Thus, a balance between osteoblastogenesis and adipogenesis that changes with aging is important for maintaining steady-state hematopoiesis.

As shown in Figure 4Ca and c, after 7 days of co-culturing $34^+38^-133^+$ cells with young and old DPMSCs, the fold increase of cells and the mean absolute numbers of $CD34^+$ cells seemed to be higher in comparison with stroma-free controls. It is of interest that there was still a tendency toward a difference between the co-cultures with young and old DPMSCs, even in the presence of a transwell. We paid attention to this difference and tried to elucidate the basic mechanisms underlying this observation. It is well documented that senescent cells secrete bioactive mediators, which negatively affect stem cell function with aging (Coppé et al., 2010). Our microarray analysis accurately extracted the *TGFB2* gene from 60,901 probes (Figure 6), which was highly expressed by old DPMSCs in comparison with young DPMSCs. We then focused on the cellular senescence induced by TGF-β2 signaling. Very interestingly, TGF-β2 significantly suppressed the growth of young DPMSCs (Figure 7B). Moreover, TGF-β2 strongly suppressed the osteogenic differentiation potential of both young and old DPMSCs (Figure 7Ca and b). Old DPMSCs produced a significantly greater amount of TGF-β2 in their cultures in comparison with young DPMSCs (Figure 7A). In addition, old DPMSCs expressed significantly higher levels of *P16* and *P21* (Figure 2C). It was also reported that TGF-β activated the p16 and p21 pathways, which induced cellular senescence (Acosta et al., 2013; van Deursen, 2014). Collectively, it is suggested that TGF-β2 can induce autocrine senescence mediated by p16 and p21. Based on these results, TGF-β2 is considered to be one of the SASP components, as recently reported (Acosta et al., 2013).

From another point of view, stem cell aging has long been considered to be irreversible. However, in this study we demonstrated that the addition of 1D11 (anti-TGF-β mAb) reversed the osteogenic differentiation potential in cultures of young and old bone-derived DPMSCs (Figure 7Cd). Thus, the suppression of TGF-β2 signaling may rejuvenate bone-derived old DPMSCs and enhance the function of young DPMSCs. It is well documented that TGF-β is an abundant bone matrix protein that affects the interaction of osteoblasts and osteoclasts (Centrella et al., 1991). Thus, TGF-β can change the balance of adipogenesis and osteogenesis *in vivo*. As recently reported, the *in vivo* administration of 1D11 increased the bone mineral density, trabecular thickness, and bone volume in mice (Edwards et al., 2010). These results were accompanied by an increase in the number of osteoblasts and a decrease in the number of osteoclasts. These findings suggest that in the near future, the administration of 1D11 that can specifically target TGF-β *in vivo* may be a therapeutic approach to the treatment of osteoporosis and other bone diseases. As shown in this study, young DPMSCs showed higher proliferative and osteogenic differentiation abilities in comparison with old DPMSCs. Thus, the *ex vivo* expansion of young DPMSCs may have a potential therapeutic advantage in comparison with the clinical application of regular batches of MSCs.

In conclusion, the present study demonstrated that old DPMSCs showed a higher adipogenic potential and lower osteogenic potential in comparison with young DPMSCs. In other words, old DPMSCs accelerated cellular senescence earlier than young DPMSCs and TGF-β2 may be partly involved in this process. Importantly, the inhibition of TGF-β signaling by 1D11 reversed this cellular senescence. These results suggest that rejuvenation of old DPMSCs may be possible through the suppression of TGF-β2 signaling.

EXPERIMENTAL PROCEDURES

Animals

The animal experiments were approved by the Animal Care Committees of Kansai Medical University. The details of the breeding and SRC assays of NOG mice are described in Supplemental Experimental Procedures.

Preparation of Human Bone Tissue-Derived Cells

The human femoral neck bone tissue samples were obtained from young and elderly patients who had undergone total hip

replacement arthroplasty. The patients' characteristics are shown in Table S1. This study was approved by the Research Ethics Committee of Kansai Medical University, and written informed consent was obtained from patients at the time of enrollment in all cases. The details of the treatment of the bone tissue specimens are described in Supplemental Experimental Procedures.

Isolation of Human Bone-Derived 11Lin$^-$CD45$^-$CD271$^{+/-}$SSEA-4$^{+/-}$ Cells by Fluorescence-Activated Cell Sorting

Human bone-derived 11Lin$^-$CD45$^-$CD271$^{+/-}$SSEA-4$^{+/-}$ cells were sorted as described previously (Matsuoka et al., 2015). The fluorescence-activated cell sorting data were processed using the FlowJo software program (FlowJo, OR, USA). The various mAbs used in this study are listed in Table S4.

Cell Culturing and Cell Proliferation Analysis

The sorted cells were seeded onto 6-well cell culture plates (BD Biosciences, CA, USA) and cultured in modified α-MEM (Nakalai Tesque, Kyoto, Japan) with 10% FBS (BioWest, Kansas City, MO, USA) and 1× Antibiotic-Antimycotic solution (Nacalai Tesque) at 37°C with 5% CO_2. For the cell proliferation assay, the cells were dissociated using 0.25% trypsin-EDTA (Thermo Fisher Scientific, Waltham, MA, USA) and seeded at a density of 2×10^4 cells per well at passage 2. During culturing, every 5 days cells were collected, counted, and reseeded at a density of 2×10^4 cells per well. At each passage, we calculated the number of population doublings based on the total number of cells.

Senescence-Associated β-Gal Assay

The details of the staining methods are described in Supplemental Experimental Procedures.

Real-Time RT-PCR

The details of the real-time RT-PCR are described in Supplemental Experimental Procedures and the primer sets used in the PCR reactions are listed in Table S5.

Analysis of the Differentiation Potentials of the Established Human Bone-Derived DPMSCs

The osteogenic, adipogenic, and chondrogenic differentiation capacities of young and old DPMSCs were assessed as described in Supplemental Experimental Procedures.

Co-culturing of 18Lin$^-$CD34$^+$CD38$^-$CD133$^+$ Cells with DPMSCs

The detailed methods that were used for the co-culturing and purification of 18Lin$^-$CD34$^+$CD38$^-$CD133$^+$ cells are described in Supplemental Experimental Procedures.

Microarray Analysis

Details of the gene expression data analysis are described in Supplemental Experimental Procedures. The microarray data were uploaded at the GEO, accession number GEO: GSE101694.

Effects of TGF-β2 and 1D11 on Proliferation and/or Differentiation of Young and Old DPMSCs

The details of the effects of TGF-β2 and 1D11 on the proliferation and/or differentiation of young and old DPMSCs are described in Supplemental Experimental Procedures.

Statistical Analysis

The statistical methods used to analyze the data are described in each of the figure legends.

SUPPLEMENTAL INFORMATION

Supplemental Information includes Supplemental Experimental Procedures, seven figures, and five tables and can be found with this article online at https://doi.org/10.1016/j.stemcr.2018.01.030.

AUTHOR CONTRIBUTIONS

H.K. designed and performed a majority of the experiments and analyzed and interpreted the data; R.N. designed and performed the experiments, analyzed and interpreted the data, and contributed to the writing of the manuscript; K.S., Y.M., and T.F. provided study material and contributed to some parts of the experiments; H.A. provided advice on the statistical analyses; H.I. contributed to the analysis and interpretation of the data; Y.S. conceived of and designed the study, analyzed and interpreted the data, provided financial and administrative support, and wrote the paper.

ACKNOWLEDGMENTS

This work was supported by Grants-in-Aid for Scientific Research C (grant nos. 21591251, 24591432, and 16K09881) from the Ministry of Education, Culture, Sports, Science and Technology (MEXT) of Japan; a grant from the Strategic Research Base Development program for Private Universities from MEXT; and MEXT-supported Program for the Strategic Research Foundation at Private Universities (S1101034 and S1201038). The authors are grateful to the Japanese Red Cross Kinki Cord Blood Bank for providing the CB samples that were used in this study.

Received: August 8, 2017
Revised: January 23, 2018
Accepted: January 24, 2018
Published: February 22, 2018

REFERENCES

Acosta, J.C., Banito, A., Wuestefeld, T., Georgilis, A., Janich, P., Morton, J.P., Athineos, D., Kang, T.W., Lasitschka, F., Andrulis, M., et al. (2013). A complex secretory program orchestrated by the inflammasome controls paracrine senescence. Nat. Cell Biol. *15*, 978–990.

Allsopp, R.C., Morin, G.B., Horner, J.W., DePinho, R., Harley, C.B., and Weissman, I.L. (2003). Effect of TERT over expression on the long-term transplantation capacity of hematopoietic stem cells. Nat. Med. *9*, 369–371.

Bethel, M., Chitteti, B.R., Srour, E.F., and Kacena, M.A. (2013). The changing balance between osteoblastgenesis and adipogenesis in aging and its impact on hematopoiesis. Curr. Osteoporos. Rep. *11*, 99–106.

Centrella, M., McCarthy, T.L., and Canalis, E. (1991). Transforming growth factor-beta and remodeling of bone. J. Bone Joint Surg. Am. *73*, 1418–1428.

Collado, M., Blasco, M.A., and Serrano, M. (2007). Cellular senescence in cancer and aging. Cell *130*, 223–233.

Coppé, J.P., Desprez, P.Y., Krtolica, A., and Campisi, J. (2010). The senescence-associated secretory phenotype: the dark side of tumor suppression. Annu. Rev. Pathol. *5*, 99–118.

Corselli, M., Chin, C.J., Parekh, C., Sahaghian, A., Wang, W., Ge, S., Evseenko, D., Wang, X., Montelatici, E., Lazzari, L., et al. (2013). Perivascular support of human hematopoietic stem/progenitor cells. Blood *121*, 2891–2901.

Edwards, J.R., Nyman, J.S., Lwin, S.T., Moore, M.M., Esparza, J., O'Quinn, E.C., Hart, A.J., Biswas, S., Patil, C.A., Lonning, S., et al. (2010). Inhibition of TGF-β signaling by 1D11 antibody treatment increases bone mass and quality in vivo. J. Bone Miner. Res. *25*, 2419–2426.

Gil, J., and Peters, G. (2006). Regulation of the INK4b-ARF-INK4a tumor suppressor locus: all for one or one for all. Nat. Rev. Mol. Cell Biol. *7*, 667–677.

Guralnik, J.M., Eisenstaedt, R.S., Ferrucci, L., Klein, H.G., and Woodman, R.C. (2004). Prevalence of anemia in persons 65 years and older in the United States: evidence for a high rate of unexplained anemia. Blood *104*, 2263–2268.

Lapidot, T., Dar, A., and Kollet, O. (2005). How do stem cells find their way home? Blood *106*, 1901–1910.

Liu, H., Xia, X., and Li, B. (2015). Mesenchymal stem cell aging: mechanisms and influences on skeletal and non-skeletal tissues. Exp. Biol. Med. (Maywood) *240*, 1099–1106.

Matsuoka, Y., Nakatsuka, R., Sumide, K., Kawamura, H., Takahashi, M., Fujioka, T., Uemura, Y., Asano, H., Sasaki, Y., Inoue, M., et al. (2015). Prospectively isolated human bone marrow cell-derived MSCs support primitive human CD34-negative hematopoietic stem cells. Stem Cells *33*, 1554–1565.

Mendelson, A., and Frenette, P.S. (2014). Hematopoietic stem cell niche maintenance during homeostasis and regeneration. Nat. Med. *20*, 833–846.

Méndez-Ferrer, S., Michurina, T.V., Ferraro, F., Mazloom, A.R., MacArthur, B.D., Lira, S.A., Scadden, D.T., Ma'ayan, A., Enikolopov, G.N., and Frenette, P.S. (2010). Mesenchymal and haematopoietic stem cells form a unique bone marrow niche. Nature *466*, 829–834.

Morrison, S.T., and Scadden, D.T. (2014). The bone marrow niche for haematopoietic stem cells. Nature *505*, 327–334.

Nakamura-Ishizu, A., and Suda, T. (2014). Aging of the hematopoietic stem cells niche. Int. J. Hematol. *100*, 317–325.

Naveiras, O., Nardi, V., Wenzel, P.L., Hauschka, P.V., Fahey, F., and Daley, G.Q. (2009). Bone-marrow adipocytes as negative regulators of the haematopoietic microenvironment. Nature *460*, 259–263.

Oh, J., Lee, Y.D., and Wagers, A.J. (2014). Stem cell aging: mechanisms, regulators and therapeutic opportunities. Nat. Med. *20*, 870–880.

Omatsu, Y., Seike, M., Sugiyama, T., Kume, T., and Nagasawa, T. (2014). Foxc1 is a critical regulator of haematopoietic stem/progenitor cell niche formation. Nature *508*, 536–540.

Pittenger, M.F., Mackay, A.M., Beck, S.C., Jaiswal, R.K., Douglas, R., Mosca, J.D., Moorman, M.A., Simonetti, D.W., Craig, S., and Marshak, D.R. (1999). Multilineage potential of adult human mesenchymal stem cells. Science *284*, 143–147.

Ren, J., Jin, P., Sabatino, M., Balakumaran, A., Feng, J., Kuznetsov, S.A., Klein, H.G., Robey, P.G., and Stroncek, D.F. (2011). Global transcriptome analysis of human bone marrow stromal cells (BMSCs) reveals proliferative, mobile, and interactive cells that produce abundant extracellular matrix proteins, some of which may affect BMSC potency. Cytotherapy *13*, 661–674.

Seeman, E., and Delmas, P.D. (2006). Bone quality—the material and structural basis of bone strength and fragility. N. Engl. J. Med. *354*, 2250–2261.

Smith, J.N., and Calvi, L.M. (2013). Concise review: current concepts in bone marrow microenvironmental regulation of hematopoietic stem and progenitor cells. Stem Cells *31*, 1044–1050.

Takahashi, M., Matsuoka, Y., Sumide, K., Nakatsuka, R., Fujioka, T., Kohno, H., Sasaki, Y., Matsui, K., Asano, H., Kaneko, K., and Sonoda, Y. (2014). CD133 is a positive marker for a distinct class of primitive human cord blood-derived CD34-negative hematopoietic stem cells. Leukemia *28*, 1308–1315.

Tormin, A., Li, O., Brune, J.C., Walsh, S., Schütz, B., Ehinger, M., Ditzel, N., Kassem, M., and Scheding, S. (2011). CD146 expression on primary nonhematopoietic bone marrow stem cells is correlated with in situ localization. Blood *117*, 5067–5077.

van Deursen, J.M. (2014). The role of senescent cells in ageing. Nature *509*, 439–446.

Wilson, A., and Trumpp, A. (2006). Bone-marrow haematopoietic-stem-cell nitches. Nat. Rev. Immunol. *6*, 93–106.

Xiao, Y., Zijl, S., Wang, L., de Groot, D.C., van Tol, M.J., Lankester, A.C., and Borst, J. (2015). Identification of the common origins of osteoclasts, macrophages, and dendritic cells in human hematopoiesis. Stem Cell Reports *4*, 984–994.